ASYMPTOTIC FEATURES OF DENSITY DISTRIBUTIONS AND FORM FACTORS FOR ^{6}Li AND ^{6}He NUCLEI WITHIN THE THREE-PARTICLE MODEL

B.E. GRINYUK, I.V. SIMENOG

Bogolyubov Institute for Theoretical Physics, Nat. Acad. of Sci. of Ukraine
(14b, Metrolohichna Str., Kyiv 03143, Ukraine; e-mail:
bgrinyuk@bitp.kiev.ua, ivsimenog@bitp.kiev.ua)

PACS 27.20.+n, 21.60.Gx, 21.10.Ft, 21.10.Gv

Asymptotic properties of structure functions for ^{6}Li and ^{6}He nuclei are studied in the framework of the model involving an α-particle and two nucleons. The density distributions of halo nucleons and the α-particle at large distances are studied and compared with analytical asymptotics. A new representation for the form factor, which is useful at low transferred momentum, has been proposed, and the asymptotic behavior of form factors has been analyzed. The results obtained demonstrate that the calculation schemes developed in the framework of the variational method with the use of a Gaussian basis allow the asymptotics of structure functions to be studied in both the coordinate and momentum spaces.

1. Introduction

Six-nucleon nuclei ($A = 6$), as was reliably established, are characterized by a distinct three-cluster structure (an α-particle plus two nucleons), so that they can be described in the framework of the three-particle model. Provided that $N\alpha$-potentials of interaction are constructed [1, 2] in such a way to reproduce not only scattering phases, but also the binding energy and the radii of nuclei under investigation, all basic structural characteristics of ^{6}Li and ^{6}He nuclei agree with the known experimental data.

To study the bound states of nuclear systems, we use precise calculation procedures based on the variational method with Gaussian basis functions. This approach has revealed a high accuracy and a reliability in its application, with a lot of problems concerning bound states in various systems of interacting particles (see work [3]), including the problem of near-threshold weakly bound states. At the same time, a natural suspicion can appear that wave functions in the Gaussian representation can have a wrong asymptotic behavior at large distances, especially for weakly bound states. In this work, we have studied with which accuracy and to which distances the Gaussian representation of wave functions is valid for finite basis dimensions. As an example, we consider the asymptotics for density distributions and form factors of weakly bound nuclei ^{6}Li and ^{6}He. In the present work, the density distributions for halo nucleons and α-particles in those nuclei at large (on the nuclear scale) distances are analyzed, and their agreement with asymptotic estimations is shown. We also study the problem of form factor asymptotics at large transferred momenta. To our knowledge, these problems, in particular, the asymptotics of density distributions, have not been solved earlier in the framework of a consecutive three-particle approach to the systems under examination. Note that, for Coulomb systems, the problem of structure function asymptotics was considered in work [4].

2. Formulation of the Problem

Nuclei ^{6}He (in the state with $J^\pi = 0^+$) and ^{6}Li (in the ground triplet state with $J^\pi = 1^+$) will be examined in the framework of the three-particle model (an α-particle plus two nucleons), as was described in works [1, 2]. The Hamiltonian of ^{6}Li nucleus in the three-particle model is used in the form

$$\hat{H} = \frac{\mathbf{p}_p^2}{2m_p} + \frac{\mathbf{p}_n^2}{2m_n} + \frac{\mathbf{p}_\alpha^2}{2m_\alpha} +$$

$$+V_{np}\left(r_{np}\right) + \hat{V}_{p\alpha}\left(r_{p\alpha}\right) + \hat{V}_{n\alpha}\left(r_{n\alpha}\right) + V_{\mathrm{C}}\left(r_{p\alpha}\right), \qquad (1)$$

T a b l e 1. Parameters of potentials $\hat{V}_{n\alpha}$ and $\hat{V}_{p\alpha}$ and calculated energies (MeV) and root-mean-square radii (Fm) of ^{6}He and ^{6}Li nuclei

Potential $V_{n\alpha}$	$E(^6\mathrm{He})$	$R_{\mathrm{ch}}(^6\mathrm{He})$	$R_m(^6\mathrm{He})$	r_{nn}	$r_{n\alpha}$	R_n	R_α
$V_0(r) = -49.813\exp(-(r/2.334)^2)$. $g = 140.0$ MeV·Fm^{-3}. $u(r) = \pi^{-3/4}\exp(-(r/2.69)^2)$	-0.973	2.068	2.589	4.398	4.221	3.252	1.208
Experiment	$-0.9734(10)$ [6]	2.068(11) [5]	2.59(5) [7]				
Potential $V_{p\alpha}$	$E(^6\mathrm{Li})$	$R_{\mathrm{ch}}(^6\mathrm{Li})$	$R_m(^6\mathrm{Li})$	r_{np}	$r_{n\alpha};\ r_{p\alpha}$	$R_n;\ R_p$	R_α
$V_0(r) = -43.605\exp(-(r/2.323)^2)$. $g = 130.0$ MeV·Fm^{-3}. $u(r) = \pi^{-3/4}\exp(-(r/2.69)^2)$	-3.699	2.560	2.553	3.192	4.201; 4.314	3.020; 3.124	1.322
Experiment	$-3.699(1)$ [6]	2.56(5) [8]	2.45(7) [9]				

where, for more generality, all three particles are assumed to have different masses and to be characterized by different pair interaction potentials. The Hamiltonian for ^{6}He nucleus has a similar form, but without the Coulomb potential V_{C}. The potentials of interaction between halo nucleons are taken in the form proposed in works [1, 2]. Such local spin-dependent potentials allow the phases of two-nucleon scattering and their low-energy parameters, as well as the basic parameters of a deuteron (the binding energy and the charge radius), to be described with a sufficient accuracy.

To describe the interaction between the nucleons and the α-particle, combined potentials $\hat{V}_{N\alpha}$, each consisting of the local and separable terms, were used as

$$\hat{V}_{N\alpha}\psi(r) = V(r)\psi(r) + gu(r)\int u(r_1)\psi(r_1)d\mathbf{r}_1, \qquad (2)$$

whose parameters were fitted with respect to the scattering phase at low energies, as well as the energies and the charge radii of ^{6}He and ^{6}Li nuclei. In this work, taking new experimental data for the charge radius of ^{6}He ($R_{\mathrm{ch},^6\mathrm{He}} = 2.068\pm0.011$ Fm [5]) into account, we use potentials with somewhat corrected parameters (Table 1). The corresponding $S_{1/2}$-phases of $N\alpha$-scattering, which were calculated on the basis of the method [2] free of the problem of singularities of the phase equation, agree with experimental results at energies lower than the breakup threshold.

The wave functions of the nuclei under study were obtained in the framework of the variational method in a Gaussian representation. They look as

$$\Phi = \hat{S}\sum_{k=1}^{K} D_k\, e^{-a_k(\mathbf{r}_1-\mathbf{r}_2)^2 - b_k(\mathbf{r}_1-\mathbf{r}_3)^2 - c_k(\mathbf{r}_2-\mathbf{r}_3)^2}. \qquad (3)$$

The appropriate accuracy of calculations is achieved, by using about 200 to 300 basis functions.

3. One-particle Density Distributions

Consider the density distributions for "point-like" particles, of which the examined nuclei are composed in the three-particle model. We assume the distributions to be normalized by 1.

The density distribution of the α-particle (more accurately, of its center of masses) $n_\alpha(r)$ has two behavior modes (Fig. 1): an internal "core" (it originates from the so-called "cigar" configuration in the three-particle wave function) transforms into an external "halo" (which is associated with the presence of the "triangle" configuration for the wave function; see works [1, 2]). It is the "triangle" configuration, the properties of which are responsible for the asymptotics of the density distribution $n_\alpha(r)$; it can be imagined as a motion of the α-particle and the deuteron cluster around their common center of masses.

Hence, when the α-particle moves far away from the center of masses of the system, the wave function ψ of ^{6}Li nucleus has a two-cluster structure and a corresponding asymptotics

$$\psi(\mathbf{r}_{np}, \boldsymbol{\rho}_\alpha) \xrightarrow[\rho_\alpha\to\infty]{} \varphi_d(r_{np})f(\rho_\alpha), \qquad (4)$$

where $\varphi_d(r_{np})$ is the wave function of a deuteron, and $f(\rho_\alpha)$ is the function of relative motion of the α-particle and the center of masses of the deuteron (the Jacobi coordinates $\mathbf{r}_{np} \equiv \mathbf{r}_p - \mathbf{r}_n$ and $\boldsymbol{\rho}_\alpha \equiv \mathbf{r}_\alpha - \frac{m_p\mathbf{r}_p + m_n\mathbf{r}_n}{m_p+m_n}$). Owing to the Coulomb repulsion between the α-particle and the deuteron, the asymptotics of $f(\rho_\alpha)$ looks like

$$f(\rho) \xrightarrow[\rho\to\infty]{} C\,(2\kappa\rho)^{-1}W_{-\eta,\,1/2}(2\kappa\rho) \xrightarrow[\rho\to\infty]{} C\,\frac{\exp(-\kappa\rho)}{(2\kappa\rho)^{1+\eta}}, \qquad (5)$$

where $W_{-\eta,\,1/2}(z)$ is the Whittaker function,

$W_{k,\mu}(z) \equiv$

$$\equiv \frac{z^k e^{-\frac{z}{2}}}{\Gamma\left(\frac{1}{2}-k+\mu\right)} \int\limits_0^\infty t^{-k-\frac{1}{2}+\mu}\left(1+\frac{t}{z}\right)^{k-\frac{1}{2}+\mu} e^{-t}dt,$$

$$W_{k,\mu}(z) \xrightarrow[|z|\to\infty,\ |arg(z)|<\pi]{} e^{-\frac{z}{2}} z^k \left(1+O\left(\frac{1}{z}\right)\right), \qquad (6)$$

$\eta = \frac{\mu_{\alpha d} Z e^2}{\hbar^2 \kappa} \approx 0.30024$ is the Coulomb parameter (for the reduced mass $\mu_{\alpha d} = \frac{m_\alpha (m_p+m_n)}{m_\alpha+m_p+m_n} \approx 1248.73172$ MeV/c^2), and $\kappa = \sqrt{\frac{2\mu_{\alpha d}|E(^6\mathrm{Li})-E(d)|}{\hbar^2}} \simeq 0.3078$ Fm^{-1}. Then, the density distribution $n_\alpha(r)$ for the α-particle is

$$n_\alpha(r) = \langle\psi|\delta\left(\mathbf{r}-(\mathbf{r}_\alpha-\mathbf{R}_{\mathrm{c.m.}})\right)|\psi\rangle =$$

$$= \lambda_\alpha^3 \int |\psi(\mathbf{r}_{np},\, \lambda_\alpha \mathbf{r})|^2\, d\mathbf{r}_{np}\,, \qquad (7)$$

where $\lambda_\alpha = \frac{m_p+m_n+m_\alpha}{m_p+m_n} \approx 2.9849318$. At large distances, taking relation (4) and the normalization condition $\int |\varphi_d(r)|^2 d\mathbf{r} = 1$ into account, it looks like

$$n_\alpha(r) \xrightarrow[r\to\infty]{} n_{\alpha,\,\mathrm{asymp}}(r) \equiv$$

$$\equiv C_\alpha\left(^6\mathrm{Li}\right) \frac{W^2_{-\eta,\,1/2}(2\lambda_\alpha\kappa r)}{(2\lambda_\alpha\kappa r)^2} \xrightarrow[r\to\infty]{}$$

$$\xrightarrow[r\to\infty]{} C_\alpha\left(^6\mathrm{Li}\right) \frac{\exp(-2\lambda_\alpha\kappa r)}{(2\lambda_\alpha\kappa r)^{2(1+\eta)}} \qquad (8)$$

with $2\lambda_\alpha\kappa \approx 1.8375$ Fm^{-1}. In Fig. 1, the calculated density distribution $n_\alpha(r)$ is shown (solid curve), and the inset demonstrates the ratio between $n_\alpha(r)$ and its asymptotics (8), namely, the combination $C_\alpha^{-1}\left(^6\mathrm{Li}\right)(2\lambda_\alpha\kappa r)^2 W^{-2}_{-\eta,\,1/2}(2\lambda_\alpha\kappa r) n_\alpha(r)$ (dashed curve). Note that the inset demonstrates the ratio between the density and its asymptotics, because the density is anomalously low at large distances. One can see that this ratio saturates already at $r \approx 2$ Fm at the asymptotic level $C_\alpha\left(^6\mathrm{Li}\right) \approx 4.88$ Fm^{-3} and remains constant up to considerable distances $r \approx 8$ Fm. This means that the calculation of $n_\alpha(r)$ (with about 300 basis Gaussian functions) is reliable up to distances of about 8 Fm, where the density becomes of the order of 10^{-9} times its values in the vicinity of zero distance. In addition, we note that the ratio $n_\alpha(r)/n_{\alpha,\mathrm{asymp}}(r)$ shown by the dashed curve has no special meaning at small distances,

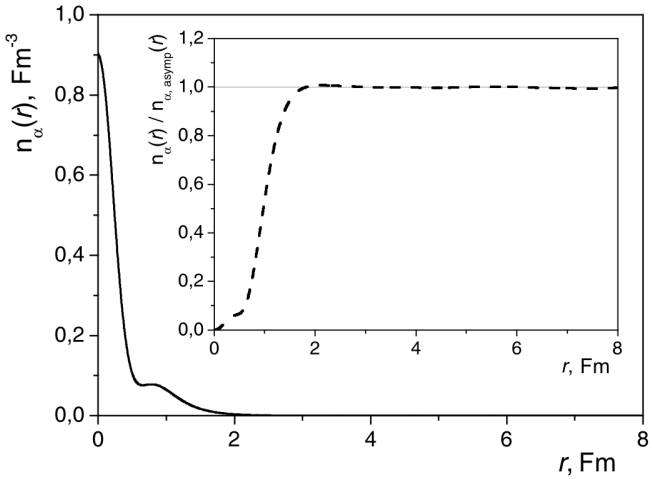

Fig. 1. Density distribution $n_\alpha(r)$ for the α-particle in ^{6}Li nucleus (solid curve). The dashed curve in the inset demonstrates the ratio between $n_\alpha(r)$ and its asymptotics $n_{\alpha,\mathrm{asymp}}(r)$ (Eq. (8))

because the asymptotic expression (8) is irrelevant in this region.

Consider the density distribution $n_p(r)$ of the halo proton in ^{6}Li nucleus,

$$n_p(r) = \langle\psi|\delta\left(\mathbf{r}-(\mathbf{r}_p-\mathbf{R}_{\mathrm{c.m.}})\right)|\psi\rangle =$$

$$= \lambda_p^3 \int |\psi(\mathbf{r}_{n\alpha},\, \lambda_p \mathbf{r})|^2\, d\mathbf{r}_{n\alpha}\,, \qquad (9)$$

where $\lambda_p = \frac{m_p+m_n+m_\alpha}{m_n+m_\alpha} \approx 1.201046$. The basic contribution to the $n_p(r)$-asymptotics at $r \to \infty$ is made by the same configuration (4). Taking the relations between the different sets of Jacobi coordinates used in expressions (4) and (9) into account, we obtain

$$\mathbf{r}_{np} = \frac{m_\alpha}{m_n+m_\alpha}\mathbf{r}_{n\alpha} + \boldsymbol{\rho}_p\,,$$

$$\boldsymbol{\rho}_\alpha = \frac{m_n(m_p+m_n+m_\alpha)}{(m_p+m_n)(m_n+m_\alpha)}\mathbf{r}_{n\alpha} - \frac{m_p}{m_p+m_n}\boldsymbol{\rho}_p, \qquad (10)$$

Eq. (4) gives rise to

$$n_p(r) \xrightarrow[r\to\infty]{}$$

$$\xrightarrow[r\to\infty]{} \sim \int \varphi_d^2\left(\lambda_p\mathbf{r} + \frac{m_\alpha}{m_n+m_\alpha}\mathbf{r}_{n\alpha}\right) \times$$

$$\times f^2\left(\frac{m_n(m_p+m_n+m_\alpha)}{(m_p+m_n)(m_n+m_\alpha)}\mathbf{r}_{n\alpha} - \frac{m_p}{m_p+m_n}\lambda_p\mathbf{r}\right) d\mathbf{r}_{n\alpha}.$$

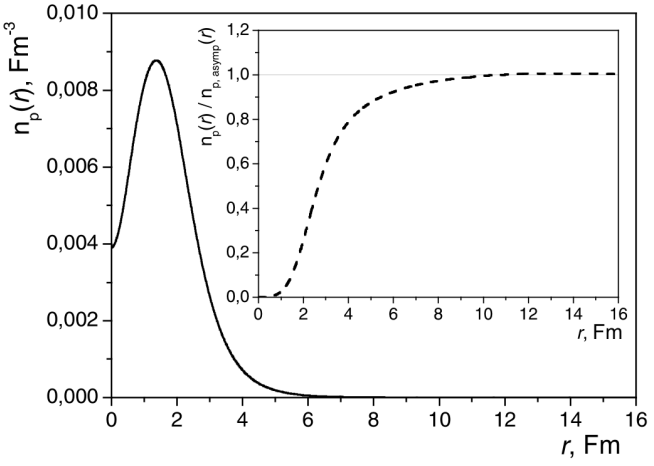

Fig. 2. Density distribution $n_p(r)$ for the halo proton in ^{6}Li nucleus (solid curve). The dashed curve in the inset demonstrates the ratio between $n_p(r)$ and its asymptotics (14)

(11)

To find the principal term in the asymptotics of expression (11), we apply the saddle-point method (or the stationary phase method). Provided that the corresponding argument remains finite as $r \to \infty$ in the decreasing functions φ_d or f, and the function itself remains constant, such two regions can provide the main contribution to the asymptotics of $n_p(r)$. In order to take the first region into account, it is convenient to introduce a new variable $\mathbf{x} \equiv \mathbf{r}_{n\alpha} + \lambda_p \frac{m_n+m_\alpha}{m_\alpha}\mathbf{r}$. For the second one, we use the substitution $\mathbf{y} \equiv \mathbf{r}_{n\alpha} - \lambda_p \frac{m_p(m_n+m_\alpha)}{m_n(m_p+m_n+m_\alpha)}\mathbf{r} = \mathbf{r}_{n\alpha} - \frac{m_p}{m_n}\mathbf{r}$. Then, in the limit $r \to \infty$, we obtain the following two main terms:

$$n_p(r) \underset{r\to\infty}{\longrightarrow}$$

$$\underset{r\to\infty}{\longrightarrow} \sim f^2\left(\frac{m_p+m_n+m_\alpha}{m_\alpha}r\right)\int \varphi_d^2\left(\frac{m_\alpha}{m_n+m_\alpha}x\right)d\mathbf{x} +$$

$$+\varphi_d^2\left(\frac{m_p}{m_n+m_n}r\right)\int f^2\left(\frac{m_n(m_p+m_n+m_\alpha)}{(m_p+m_n)(m_n+m_\alpha)}y\right)d\mathbf{y}, \tag{12}$$

in which both integrals converge. Independent of the short-range potential model asymptotics of the deuteron wave function is known to be

$$\varphi_d(r) \underset{r\to\infty}{\longrightarrow} C_d \frac{\exp(-\alpha r)}{\alpha r}, \tag{13}$$

where the coefficient C_d is directly connected with the asymptotic normalization constant A_S of the deuteron (for the selected potential, $A_S = \frac{\sqrt{4\pi}}{\alpha}C_d \approx 0.88$ Fm$^{-1/2}$), the value $\alpha = \sqrt{\frac{2\mu_{np}\varepsilon_d}{\hbar^2}} \approx 0.23163$ Fm^{-1} ($\mu_{np} = \frac{m_n m_p}{m_n+m_p}$, $\varepsilon_d = 2.224756$ MeV). Using also asymptotics (5) for $f(\rho)$, we transform Eq. (12) into

$$n_p(r) \underset{r\to\infty}{\longrightarrow}$$

$$\underset{r\to\infty}{\longrightarrow} C_{p1}\left(^6\mathrm{Li}\right)\left(2\Lambda_{p1}\kappa r\right)^{-2} W^2_{-\eta,\,1/2}\left(2\Lambda_{p1}\kappa r\right) +$$

$$+ C_{p2}\left(^6\mathrm{Li}\right)\left(2\Lambda_{p2}\alpha r\right)^{-2}\exp\left(-2\Lambda_{p2}\alpha r\right), \tag{14}$$

where $\Lambda_{p1} \equiv \frac{m_p+m_n+m_\alpha}{m_\alpha} \approx 1.5037956$ and $\Lambda_{p2} \equiv \frac{m_p+m_n}{m_n} \approx 1.99862348$. We keep both terms in asymptotics (14), because, in this problem, the coincidence of parameters, $\Lambda_{p1}\kappa \approx \Lambda_{p2}\alpha$, is observed with an accuracy high for nuclear physics ($\Lambda_{p1}\kappa \approx 0.46286$ Fm^{-1} and $\Lambda_{p2}\alpha \approx 0.46294$ Fm^{-1}). As a result, none of terms in asymptotics (14) for $n_p(r)$ can be neglected in a wide interval of distances that are considered. Note that the coincidence $\Lambda_{p1}\kappa \approx \Lambda_{p2}\alpha$, when expressed in another form, means that

$$E\left(^6\mathrm{Li}\right) \approx \frac{(m_p+m_n)(m_n+m_\alpha)}{m_n(m_p+m_n+m_\alpha)}E(d) \approx \frac{5}{3}E(d). \tag{15}$$

We should emphasize that Eq. (15) does not establish an analytical dependence between three- and two-particle energies and particle masses. It only reflects a coincidence of some combinations made up of specific physical constants. Comparing Eq. (14) with the calculated density $n_p(r)$, we can determine the coefficients $C_{p1}\left(^6\mathrm{Li}\right)$ and $C_{p2}\left(^6\mathrm{Li}\right)$. As is seen from Fig. 2, the asymptotics in form (14) with the coefficients $C_{p1}\left(^6\mathrm{Li}\right) = 0.565$ Fm^{-3} and $C_{p2}\left(^6\mathrm{Li}\right) = 0.250$ Fm^{-3} is achieved starting from the distances $r \approx 10$ Fm and, then, coincides with the calculated density. The density distribution $n_p(r)$ found numerically (with 300 basis functions) turns out reliable up to larger distances $r \approx 16$ Fm, where the magnitudes of $n_p(r)$ are about 10^{-7} times its maximum value.

We emphasize that an essential decrease of the density distribution $n_p(r)$, as well as $n_n(r)$, at short distances is associated with the repulsion between halo nucleons at small distances and a substantial role of the "triangle" configuration in ^{6}Li nucleus, in which the center of masses of the deuteron cluster is located aside from the center of masses of the nucleus.

In a similar way, one can obtain an asymptotics of the density distribution $n_n(r)$ for a halo neutron in ^{6}Li nucleus:

$$n_n(r) \underset{r\to\infty}{\longrightarrow}$$

$$\underset{r\to\infty}{\longrightarrow} C_{n1}\left(^6\mathrm{Li}\right)\left(2\Lambda_{n1}\kappa r\right)^{-2} W^2_{-\eta,\,1/2}\left(2\Lambda_{n1}\kappa r\right) +$$

$$+C_{n2}\left(^6\mathrm{Li}\right)\left(2\Lambda_{n2}\alpha r\right)^{-2}\exp\left(-2\Lambda_{n2}\alpha r\right), \qquad (16)$$

where $\Lambda_{n1} = \Lambda_{p1}$, and $\Lambda_{n2} \equiv \frac{m_p+m_n}{m_p} \approx 2.0013784$. Since $\Lambda_{n2}\alpha \approx 0.46358$ Fm^{-1}, we have almost the same coincidence relation, $\Lambda_{n1}\kappa \approx \Lambda_{n2}\alpha$, as it was in the previous case. Therefore, both terms in Eq. (16) give comparable contributions to the asymptotics of the distribution $n_n(r)$ in a wide interval of distances under consideration. Comparing asymptotics (16) with the calculated distribution $n_n(r)$, we find that $C_{n1}\left(^6\mathrm{Li}\right) = 0.475$ Fm^{-3} and $C_{n2}\left(^6\mathrm{Li}\right) = 0.222$ Fm^{-3}.

Since the distribution of neutrons in ^{6}Li nucleus [2] differs weakly from that of protons (see Fig. 2), we present the ratio n_p/n_n in Fig. 3. This ratio should tend to a constant at large distances, because the first (principal) terms in asymptotic expressions (14) and (16) differ from each other by only a factor. The other terms, although being important at intermediate distances, differ weakly in both expressions by exponents in exponential functions. So, the ratio n_p/n_n should achieve the constant value rather quickly. As is seen from Fig. 3, starting from distances of about 6 Fm, this ratio approaches a constant of about 1.18. It is larger than 1 because the halo proton in ^{6}Li, owing to Coulomb repulsion from the α-particle, is located somewhat farther from the nuclear center than the neutron, whereas $n_p < n_n$ at short distances.

The structure of ^{6}He nucleus, to a great extent, is similar to that of ^{6}Li one [1, 2] at distances within several Fm, but the asymptotic behaviors of the density distribution of halo neutrons and α-particles in those nuclei are different. It is connected with the fact that ^{6}He nucleus has a three-particle breakup threshold ($^6\mathrm{He} \to n + n + \alpha$) rather than a two-particle one, as ^{6}Li does ($^6\mathrm{Li} \to d + \alpha$). Therefore, the wave function of ^{6}He has a three-particle Merkuriev asymptotics [10, 11] of the type $\sim \frac{\exp\left(-\sqrt{|E|}R\right)}{R^{5/2}}$, where R is the hyperradius. For a more detailed analysis of the asymptotics of the density distribution $n_\alpha(r)$ for the α-particle in ^{6}He nucleus, let us consider the wave function Φ of this system in the three-particle model (with the momentum $L = 0$)

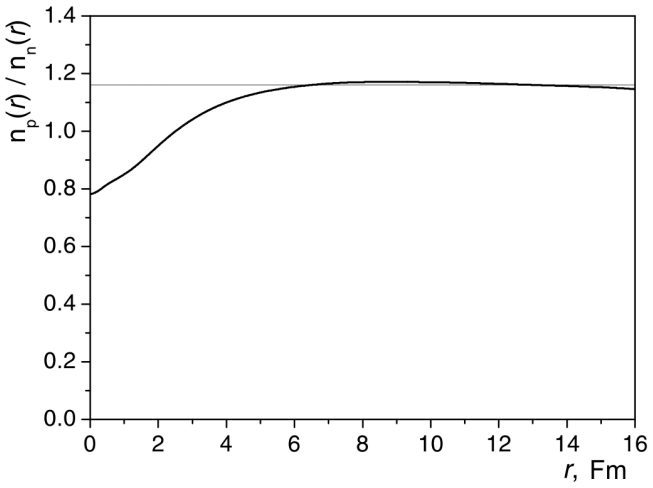

Fig. 3. The density distribution ratio $n_p(r)/n_n(r)$ for halo nucleons in ^{6}Li nucleus

in terms of the variables r_{nn} (the distance between neutrons), ρ_α (the distance from the α-particle to the center of masses of two neutrons), and θ (the angle between the vectors $\mathbf{r}_{nn}$ and $\boldsymbol{\rho}_\alpha$). Beyond the region of interaction between particles, the function $\Phi(r_{nn}, \rho_\alpha, \theta)$ looks like

$$\Phi(r_{nn}, \rho_\alpha, \theta) = \sum_{l=0}^{\infty} P_l\left(\cos\theta\right)\Psi_l\left(r_{nn}, \rho_\alpha\right). \qquad (17)$$

Let us change over to the variables $s_{12} = \sqrt{\mu_{nn}}r_{nn}$ and $s_3 = \sqrt{\mu_{(2n)\alpha}}\rho_\alpha$ and write down the Schrödinger equation in the asymptotic region (without interaction) for the single zero-order term $\Psi_0(s_{12}, s_3)$ of expansion (17). Introducing $\varphi(s_{12}, s_3) \equiv s_{12}s_3\Psi_0(s_{12}, s_3)$, we obtain the equation

$$-\left(\frac{\partial^2}{\partial s_{12}^2} + \frac{\partial^2}{\partial s_3^2}\right)\varphi = -\varkappa^2\varphi, \qquad (18)$$

where $-\varkappa^2 \equiv 2E\left(^6\mathrm{He}\right)/\hbar^2$. In terms of the variables R and α, where $s_{12} = R\cos\alpha$ and $s_3 = R\sin\alpha$ (similar variables were used by V. Efimov in [12]), we obtain the following equation for the function $u \equiv \sqrt{R}\varphi$:

$$\frac{\partial^2 u}{\partial R^2} + \frac{1}{R^2}\left(\frac{\partial^2}{\partial\alpha^2} + \frac{1}{4}\right)u = \varkappa^2 u. \qquad (19)$$

The solution of this equation that vanishes at large distances (at $\rho_\alpha \to \infty$, so that $R \to \infty$ simultaneously, because $R = \sqrt{\mu_{nn}r_{nn}^2 + \mu_{(2n)\alpha}\rho_\alpha^2}$) is the function

$$u\left(R, \alpha\right) = C\exp\left(-\varkappa R\right)\sin\left(\frac{\alpha}{2} + \delta\right) \qquad (20)$$

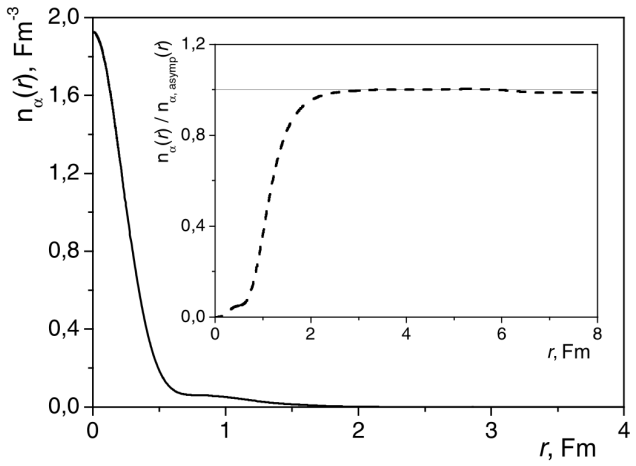

Fig. 4. Density distribution $n_\alpha(r)$ for the α-particle in ^{6}He nucleus (solid curve). The dashed curve in the inset demonstrates the ratio between $n_\alpha(r)$ and its asymptotics $n_{\alpha,\mathrm{asymp}}(r)$ (Eq. (23))

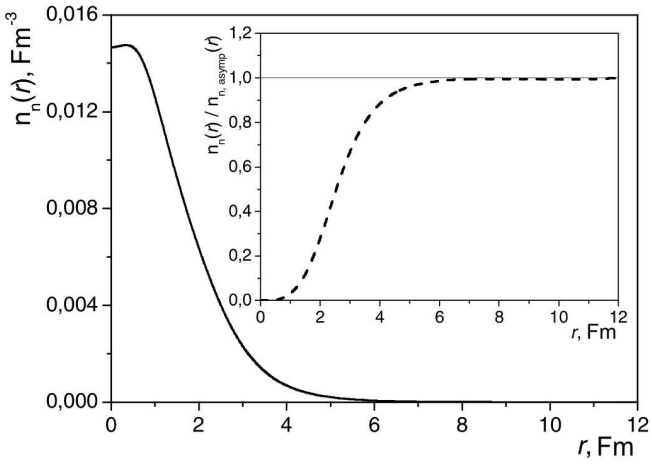

Fig. 5. Density distribution $n_n(r)$ for the halo proton in ^{6}He nucleus (solid curve). The dashed curve in the inset demonstrates the ratio between $n_n(r)$ and its asymptotics (24)

with an arbitrary δ. Returning to the initial variables, we have the following dependence for Ψ_0 in the asymptotic region:

$$\Psi_0(r_{nn},\rho_\alpha) \sim \frac{\exp\left(-\varkappa\sqrt{\mu_{nn}r_{nn}^2+\mu_{(2n)\alpha}\rho_\alpha^2}\right)}{r_{nn}\rho_\alpha\left(\mu_{nn}r_{nn}^2+\mu_{(2n)\alpha}\rho_\alpha^2\right)^{1/4}}\times$$

$$\times\sin\left(\frac{1}{2}\arctan\left(\sqrt{\frac{\mu_{(2n)\alpha}}{\mu_{nn}}}\frac{\rho_\alpha}{r_{nn}}\right)+\delta\right). \qquad (21)$$

This expression gives its contribution to the asymptotics of the density distribution $n_\alpha(r)$ in ^{6}He nucleus. Substituting expression (21) into Eq. (7)—where λ_α should be replaced by $\tilde\lambda_\alpha \equiv \frac{2m_n+m_\alpha}{2m_n} \approx 2.98356566$ in the case of ^{6}He nucleus—we obtain the following estimation as $\rho_\alpha \to \infty$:

$$\int\left|\Psi_0\left(r_{nn},\tilde\lambda_\alpha r\right)\right|^2 d\mathbf{r}_{nn} \underset{\rho_\alpha\to\infty}{\longrightarrow}$$

$$\underset{\rho_\alpha\to\infty}{\longrightarrow} \sim \frac{e^{\left(-2\varkappa\sqrt{\mu_{(2n),\alpha}}\,\rho_\alpha\right)}}{\rho_\alpha^3}\times$$

$$\times\int\frac{e^{\left(-2\varkappa\left(\sqrt{\mu_{nn}r_{nn}^2+\mu_{(2n),\alpha}\rho_\alpha^2}-\sqrt{\mu_{(2n),\alpha}}\,\rho_\alpha\right)\right)}}{r_{nn}^2}d\mathbf{r}_{nn}\underset{\rho_\alpha\to\infty}{\longrightarrow}$$

$$\underset{\rho_\alpha\to\infty}{\longrightarrow} \sim \frac{e^{\left(-2\varkappa\sqrt{\mu_{(2n),\alpha}}\,\rho_\alpha\right)}}{\rho_\alpha^3}\times$$

$$\times\int_0^\infty\exp\left(-\frac{\varkappa\mu_{nn}r_{nn}^2}{\sqrt{\mu_{(2n),\alpha}}\,\rho_\alpha}\right)dr_{nn}\underset{\rho_\alpha\to\infty}{\longrightarrow}$$

$$\underset{\rho_\alpha\to\infty}{\longrightarrow} \sim \frac{e^{\left(-2\varkappa\sqrt{\mu_{(2n),\alpha}}\,\tilde\lambda_\alpha r\right)}}{r^{5/2}}. \qquad (22)$$

It is clear that the asymptotics of $n_\alpha(r)$ involves the next terms of the expansion in the reciprocal distance as well:

$$n_\alpha(r) \underset{r\to\infty}{\longrightarrow} \frac{e^{-ar}}{(ar)^{5/2}}\left(C_{\alpha0}+\frac{C_{\alpha1}}{ar}+...\right). \qquad (23)$$

Here, $a \equiv 2\varkappa\sqrt{\mu_{(2n),\alpha}}\tilde\lambda_\alpha \approx 1.49133$ Fm^{-1}. When comparing expression (23) with the result of calculations of the density distribution (see Fig. 4), we have to consider, besides the first term of expansion, also the second one, because the constant $C_{\alpha0} = 0.10$ Fm^{-3} turns out small in comparison with $C_{\alpha1} = 2.43$ Fm^{-3}, and both terms are important at intermediate r. One can see that asymptotics (23) is valid starting from $r \approx 2$ Fm, and numerical calculations (with about 350 basis functions) confirm its validity to distances $r \approx 8$ Fm, where $n_\alpha(r)$ gets values of the order of 10^{-9} times those at zero distances.

Consider the asymptotics of the halo-neutron density distribution $n_n(r) = \langle\psi|\delta\left(\mathbf{r}-(\mathbf{r}_n-\mathbf{R}_{\mathrm{c.m.}})\right)|\psi\rangle$ in ^{6}He nucleus. Using the calculation scheme like (22), we obtain (a similar asymptotics is valid for three-nucleon nuclei as well [13])

$$n_n(r) \underset{r\to\infty}{\longrightarrow} \frac{e^{-br}}{(br)^{5/2}}\left(C_{n0}+\frac{C_{n1}}{br}+...\right), \qquad (24)$$

where $b \equiv 2\varkappa\sqrt{2m_n} \approx 0.61303$ Fm^{-1}. Comparing the asymptotic expression (24) with the result of calculations of $n_n(r)$ for ^{6}He nucleus (see Fig. 5), we find that $C_{n0} = 0.04$ Fm^{-3} and $C_{n1} = 0.11$ Fm^{-3}. One can see that asymptotics (24) holds true starting from distances of about 6 Fm and remains reliable up to distances of about 12 Fm (calculations with 250 basis functions symmetrized with respect to the permutation of halo-neutron coordinates).

Hence, the asymptotics of wave functions and density distributions can be studied taking advantage of variational calculations with the Gaussian basis. Such calculations provide a reliable base for the determination of asymptotic constants. The asymptotics of density distributions have, to a large degree, a universal character, because they were examined in the region, where nuclear interaction does not manifest itself.

4. Form Factors for Low Transferred Momenta

The charge form factors of ^{6}Li and ^{6}He nuclei are known to have a characteristic "dip" at a certain $q^2_{\min}$ ($q^2_{\min} \approx 8.3$ Fm^{-2} for ^{6}Li and ≈ 10.1 Fm^{-2} for ^{6}He). Recall that the form factors of nuclei consisting of non-point particles (nucleons and α-particles) can be expressed as follows:

$$F_{\mathrm{ch},^6\mathrm{He}}(q) = F_{\alpha,^6\mathrm{He}}(q) F_{\mathrm{ch},^4\mathrm{He}}(q),$$

$$F_{\mathrm{ch},^6\mathrm{Li}}(q) = \frac{2}{3} F_{\alpha,^6\mathrm{Li}}(q) F_{\mathrm{ch},^4\mathrm{He}}(q) + \frac{1}{3} F_p(q) f_p(q), \qquad (25)$$

where $F_\alpha(q) \equiv \int e^{-i(\mathbf{qr})} n_\alpha(r) d\mathbf{r}$ is the form factor of a "point-like" α-particle in the relevant nucleus, $F_{\mathrm{ch},^4\mathrm{He}}(q)$ is the characteristic charge form factor of the α-particle, $F_p(q) \equiv \int e^{-i(\mathbf{qr})} n_p(r) d\mathbf{r}$ is the form factor of the "point-like" halo proton in ^{6}Li nucleus, and $f_p(q)$ is the form factor of the proton itself. The presence of the "dip" in the charge form factor of ^{6}He nucleus, as well as its position, is associated with properties of the characteristic form factor of the α-particle, whereas $F_\alpha(q)$ is a smoothly decreasing function without any dips. A substantial contribution to the charge form factor of ^{6}Li nucleus is also given by the second term in expression (25) which contains the proton form factor.

Consider the form factor of the "point-like" proton in the ^{6}Li halo. At low transferred momenta,

$$F_p(q^2) \underset{q\to 0}{\longrightarrow} 1 - \frac{1}{6}\left\langle r_p^2 \right\rangle q^2 + \frac{1}{120}\left\langle r_p^4 \right\rangle q^4 + \ldots =$$

$$= \sum_{k=0}^{\infty} \frac{(-1)^k}{(2k+1)!} \left\langle r^{2k} \right\rangle q^{2k}, \qquad (26)$$

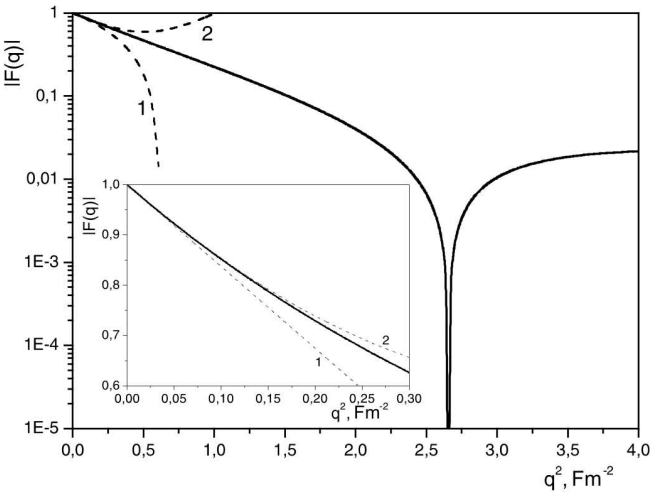

Fig. 6. Form factor $F_p(q)$ of the "point-like" halo proton for ^{6}Li nucleus (solid curve) in the range of low transferred momenta q^2. Curves *1* and *2* are approximation (26) with two and three terms, respectively. The inset demonstrates the range of very low q^2

where $\left\langle r_p^2 \right\rangle^{1/2} = R_p \approx 3.124$ Fm is the root-mean-square radius for the halo proton (see Table 1), and $\left\langle r_p^4 \right\rangle^{1/4} = \left(\int r^4 n_p(r) d\mathbf{r}\right)^{1/4} \approx 3.725$ Fm (this value was obtained by direct calculations using the density distribution $n_p(r)$ in ^{6}Li nucleus).

As Fig. 6 demonstrates, the formal expansion (26) is inconvenient for studying the form factors at low transferred momenta, in particular, for a reliable determination of root-mean-square radii directly from form-factor curves, because the terms of series (26) quickly grow with the momentum transferred, whereas the form factor quickly falls down. As a result, expansion (26) coincides with the form factor only at anomalously small q^2. We suggest the expansion in the following form:

$$F_p\left(q^2\right) \approx \frac{1 - \frac{q^2}{q^2_{\min}}}{1 + S_2 q^2 + S_4 q^4 + \ldots},$$

$$S_2 \equiv \frac{R_p^2}{6} - \frac{1}{q^2_{\min}},$$

$$S_4 \equiv \frac{R_p^2}{6}\left(\frac{R_p^2}{6} - \frac{1}{q^2_{\min}}\right) - \frac{\left\langle r^4 \right\rangle}{120}, \qquad (27)$$

where the factor $1 - q^2/q^2_{\min}$, which makes allowance for the "dip" in the form factor, is singled out explicitly, and the expansion in a series of q^2 (up to q^4) is carried

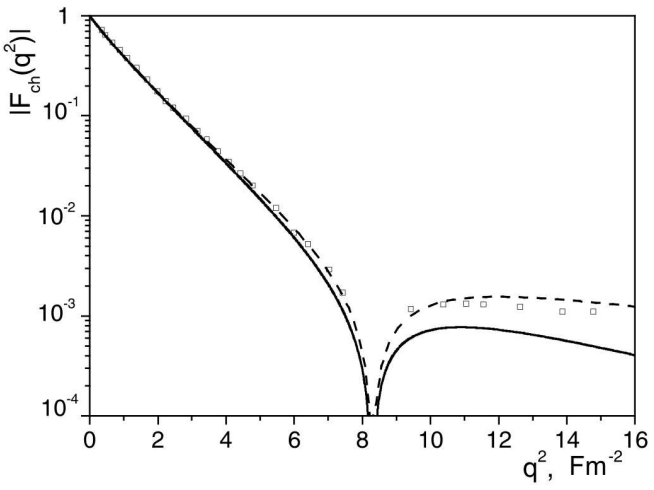

Fig. 7. Charge form factor $F_{\rm ch}(q)$ of ^{6}Li nucleus (solid curve) and representation (28) (dashed curve). Experimental values (without experimental errors) are denoted by squares

out in the denominator. Expression (27) has the same expansion in a series of q^2 (up to q^4 inclusive), as formula (26) does, but it describes the form factor at low transferred momenta much better and even in the "dip" region ($0 \le q^2 \le q^2_{\rm min} \approx 2.64$ Fm^{-2}). Note that, if there are more "dips" in the form factor, it is better to single out all of them explicitly as multipliers, as it was done in the numerator of formula (27). It is evident that, if the form factor is "dip-free", it is more convenient to expand just the reciprocal form factor in a series of squared transferred momentum.

The proposed expansion (27) allows one to expand the appropriate q^2-region to make the determination of the parameter $\langle r^2\rangle^{1/2}$ more reliable and to evaluate the quantity $\langle r^4\rangle^{1/4}$ directly from experimental curves for form factors. If the charge form factor of ^{6}Li nucleus is considered at small and medium q^2 before the "dip" region, an expansion of type (27) should contain more terms for the description of the form factor at these q^2 to be correct. It is explained by the fact that, in this case, $q^2_{\rm min}$ is considerably larger, being of about 8.3 Fm^{-2}. In Fig. 7, we compare the experimental form factor with that given by the expression

$$F_{{\rm ch},^6{\rm Li}}(q) \approx \frac{1-\frac{q^2}{q^2_{\rm min}}}{1+\tilde S_2 q^2+\tilde S_4 q^4+\tilde S_6 q^6+\tilde S_8 q^8},$$

$$\tilde S_2 \equiv \frac{R^2_{\rm ch}}{6}-\frac{1}{q^2_{\rm min}},$$

$$\tilde S_4 \equiv \frac{R^2_{\rm ch}}{6}\left(\frac{R^2_{\rm ch}}{6}-\frac{1}{q^2_{\rm min}}\right)-\frac{\langle r^4\rangle_{\rm ch}}{120},$$

$$\tilde S_6 \equiv \frac{\langle r^6\rangle_{\rm ch}}{7!}+2\tilde S_2\tilde S_4-\tilde S_2^3+\left(\tilde S_4-\tilde S_2^2\right)\frac{1}{q^2_{\rm min}},$$

$$\tilde S_8 \equiv \tilde S_2^4+\tilde S_4^2+2\tilde S_2\tilde S_6-3\tilde S_2^2\tilde S_4+$$

$$+\left(\tilde S_2^3+\tilde S_6-2\tilde S_2\tilde S_4\right)\frac{1}{q^2_{\rm min}}-\frac{\langle r^8\rangle_{\rm ch}}{9!} \qquad (28)$$

and with the result of straightforward calculations of the charge form factor for ^{6}Li. The expansion of expression (28) in a q^2-series coincides with expansion (26) to an accuracy of the q^8-term inclusive. In expression (28), the experimental parameters are $q^2_{\rm min} \approx 8.3$ Fm^{-2} and $R_{\rm ch} = 2.56$ Fm [7], whereas the parameters $\langle r^4\rangle^{1/4}_{\rm ch} = 3.19$ Fm, $\tilde S_6 = 0.07$ Fm^6, and $\tilde S_8 = 0.006$ Fm^8 were fitted to put the form factor curve in agreement with experiment. The straightforward calculation of the parameter $\langle r^4\rangle^{1/4}_{\rm ch} \approx 3.15$ Fm using the charge density of ^{6}Li nucleus gives rise to a result that is close to that obtained when fitting the form factor curve. Hence, an expansion of type (28) makes it possible to determine not only the parameter $R_{\rm ch}$, but even the quantity $\langle r^4\rangle^{1/4}_{\rm ch}$, using the experimental curve for the form factor. At the same time, the application of expansion in form (26) generates considerable errors even for $R_{\rm ch}$. Note that, owing to its form, representation (28), as is seen from Fig. 7, is capable of reproducing the experimental form factor even in the region behind the "dip".

Should the experimental charge form factor for ^{6}He nucleus be known, it would be possible to obtain an estimation for $\langle r^4\rangle^{1/4}_{\rm ch}$ in this case as well and to compare it with the value $\langle r^4\rangle^{1/4}_{\rm ch} \approx 2.39$ Fm, which follows from direct calculations using the charge density for this nucleus. It is of interest that an approximation of type (28) with the parameters given above for $R_{{\rm ch},^6{\rm He}}$, $\langle r^4\rangle^{1/4}_{{\rm ch},^6{\rm He}}$, and $q^2_{\rm min}$, as well as $S_6 = 0.02$ Fm^6 and $S_8 = 0.003$ Fm^8, practically coincides with the form factor calculated for the range of low and medium q^2, which is illustrated in Fig. 8.

Recall that the charge radius of ^{6}He is substantially less than the similar parameter of ^{6}Li nucleus (though their mass radii are close), because the ^{6}Li halo contains a proton, which contributes to the charge density distribution of this nucleus together with the α-particle,

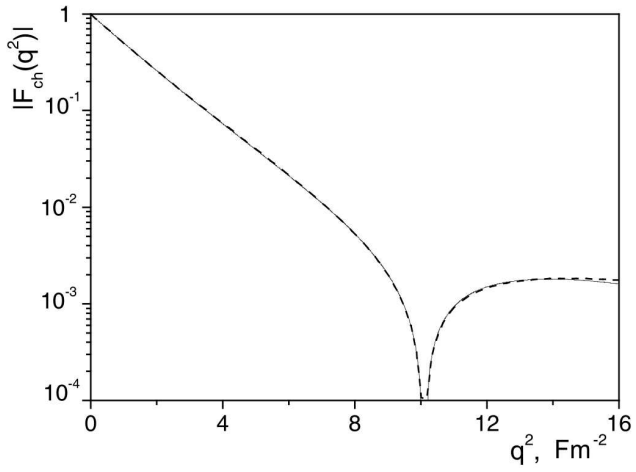

Fig. 8. Calculated charge form factor of ^{6}He nucleus (solid curve) in comparison with the approximation of type (28) (dashed line)

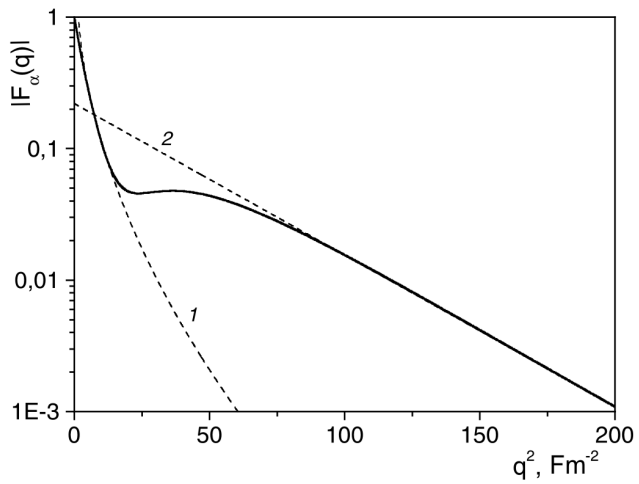

Fig. 9. Calculated form factor $F_\alpha(q)$ for the α-particle in ^{6}Li nucleus (solid curve) in the range of the transferred momenta $q^2 \leq 200$ Fm^{-2}. Dashed curve *1* corresponds to asymptotics (32), and dashed curve *2* to interpolation curve $\sim \exp\left(-0.0265q^2\right)$

whereas the charge radius of ^{6}He stems only from the α-particle motion (and its own charge distribution). For the same reason, $\langle r^4\rangle^{1/4}_{\mathrm{ch},^6\mathrm{He}} < \langle r^4\rangle^{1/4}_{\mathrm{ch},^6\mathrm{Li}}$ (see Table 2). Note also that, in all considered cases, $\langle r^2\rangle^{1/2} < \langle r^4\rangle^{1/4}$ owing to the inequality

$$\left(\int r^2 n(r) d\mathbf{r}\right)^2 < \int r^4 n(r) d\mathbf{r}, \tag{29}$$

which is a particular case of the Cauchy–Buniakowski–Schwarz inequality for the functions $f(r) \equiv r^2\sqrt{n(r)}$ and $g(r) \equiv \sqrt{n(r)}$, with regard for the normalization condition $\int n(r) d\mathbf{r} = 1$.

T a b l e 2. Calculated charge radii and $\langle r^4\rangle^{1/4}_{\mathrm{ch}}$ for ^{6}Li and ^{6}He nuclei

Nucleus	R_{ch}, Fm	$\langle r^4\rangle^{1/4}_{\mathrm{ch}}$, Fm
^{6}Li	2.560	3.15
^{6}He	2.068	2.39

5. Form Factor Asymptotics Problem

The study of the asymptotics of form factors of complex nuclear systems at large transferred momenta (they correspond to short distances in the coordinate space) can be important for the analysis of both interparticle interactions at small distances and the structure of particles of the system. In our model of ^{6}Li and ^{6}He nuclei, both the interaction and the structure of particles-constituents are considered at the phenomenological level.

The asymptotics of form factors in complex nuclear systems were studied in a number of works [14–18] in the framework of the non-relativistic approach and for certain interaction potentials. The final result of those researches consists in that the form factors for systems with three identical particles are determined in terms of Fourier components of interaction potentials $v(q)$ in the form

$$F(q) \sim \left(\frac{v(q)}{q^2}\right)^2, \tag{30}$$

provided that the law of potential decrease at large momenta satisfies the conditions

$$v(q)\, q^{1+\varepsilon} \to 0, \quad v(q)\, \exp\left(aq^{1-\varepsilon}\right) \to \infty\,. \tag{31}$$

The Gaussian potentials used in this work do not satisfy the second of these conditions.

Even if the consideration is confined to the non-relativistic approximation with the potentials chosen as a combination of gaussoids (with the local and non-local terms for $N\alpha$-interaction), the analysis of the form factor asymptotics is not simple and cannot be reduced to a simple generalization of the results of works [14–16] (see also work [17] for nuclei considered as Fermi systems) valid in the case of power-law (in the momentum representation) interaction potentials.

Let us consider ^{6}Li nucleus and the form factor $F_\alpha(q)$ for the "point-like" α-particle in this nucleus. The corresponding form factor $F_\alpha(q)$ calculated in the framework of the three-particle model is shown in Fig. 9. One

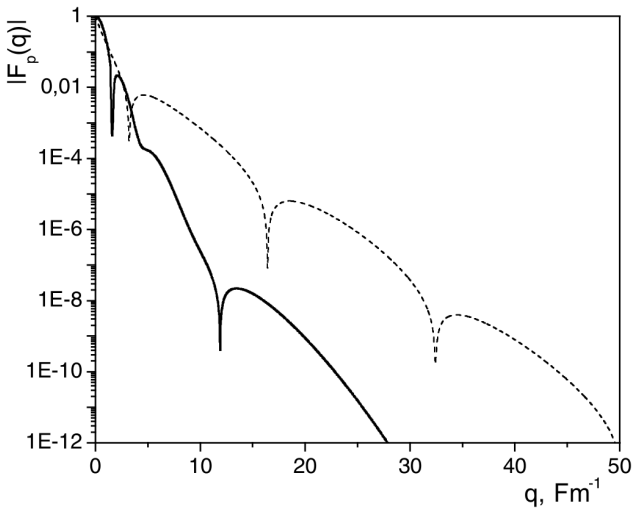

Fig. 10. Calculated form factor $F_p(q)$ of the halo proton in ^{6}Li nucleus (solid curve) in comparison with the calculated form factor $F_{p(d)}(q)$ of the proton in a deuteron (dashed curve)

can distinguish between two modes of form factor behavior (similarly to the momentum distribution for the α-particle in ^{6}Li nucleus [2]) depending on the squared transferred momentum, and such a dependence turns out to be rather a slowly decreasing function. It can be explained by the fact that the interaction between the α-particle and the deuteron cluster is governed (at the qualitative level) by a doubled potential $V_{N\alpha}$, which includes a local attraction in the form of a gaussoid and a separable (of the first rank) repulsion with a Gaussian form factor. Then, in the two-particle approximation (α-particle plus deuteron) for this potential, we can demonstrate that the form factor asymptotics (similarly to the two-particle wave function in the momentum space) diminishes like

$$F(q) \sim$$

$$\sim \frac{1}{q+q_0}\,\exp(-\lambda(q+p_0)\sqrt{\ln\left(\beta\left((q+p_0)^2+a^2\right)\right)}\,). \quad (32)$$

From Fig. 9, one can see that the form factor $F_\alpha(q)$ has a very similar behavior (dashed curve *1*) in the real three-particle calculation as well, at $q^2 \le 10$ Fm^{-2} (in the range of transferred momenta which is associated with the "triangle" configuration). The matter is that the average kinetic energy of the α-particle in ^{6}Li nucleus is about 3 MeV [2], which corresponds to $q^2 \approx 0.6$ Fm^{-2}. Therefore, the region $q^2 \le 10$ Fm^{-2} could be considered as asymptotic, were it not for the anomalous change of behavior modes due to the "cigar" configuration. If the problem had been a genuine two-particle one with a Gaussian attraction potential, it would have been possible to present explicit expressions for the parameters in expression (32) in terms of the potential radius and the intensity (in particular, λ would have been proportional to the gaussoid radius). Since we actually deal with a more complicated (three-particle) problem, and expression (32) rather only resembles the real asymptotics, we should fit the parameters in expression (32). A comparison with the calculated curve brings about $\lambda \approx 0.377$ Fm and $\beta \approx 0.7$ Fm^2. The other parameters, except for the multiplier, weakly affect the asymptotic curve. Therefore, for simplicity, we put $q_0 = 1$ Fm^{-1}, $p_0 = 0$ Fm^{-1}, and $a^2 = 1$ Fm^{-2}.

At larger transferred momenta ($q^2 \ge 50$ Fm^{-2}), another mode, which is governed by the "cigar" configuration, reveals itself in the asymptotics of the form factor $F_\alpha(q)$. The central part of the density distribution $n_\alpha(r)$, which is similar to a small-radius gaussoid (see Fig. 1), is responsible for this contribution to the form factor asymptotics. Therefore, its Fourier transform is also very similar to a gaussoid (in Fig. 9, this region of the form factor is interpolated by dashed curve *2* which diminishes following the law $\sim \exp(-0.0265q^2)$). However, at very large q^2 lying beyond the reach of our calculation that achieves $q^2 \sim 600$ Fm^{-2} at about 300 basis functions, this dependence must concede the true asymptotics of type (32), originating from the "triangle" configuration, because the latter decreases slower. Dashed curves *1* and *2* in Fig. 9 intersect at $q^2 \sim 1500$ Fm^{-2} which is located beyond the validity range of the nonrelativistic potential model.

We now consider the form factor $F_p(q)$ of the halo proton in ^{6}Li nucleus (not taking the structure of the proton itself into account). In Fig. 10, the calculated form factor $F_p(q)$ is depicted (solid curve), the structure of which, besides "dips", demonstrates the change of slope (in the range $q \approx 5$ Fm^{-1}). Such a change is again explained by the fact that the "triangle" configuration manifests itself in the form factor behavior at $q \le 5$ Fm^{-1}, and the "cigar" configuration at $q \ge 5$ Fm^{-1}.

To explain the characteristic behavior of $F_p(q)$ at a qualitative level, one may admit that the main contribution to the asymptotics is given by the "triangle" configuration, in which the α-particle and the deuteron cluster move around their common center of masses. This is related not only to the fact that the probability of this configuration in ^{6}Li nucleus is higher [2] than the probability of the "cigar" configuration, but also because, just in this configuration, the short-range interaction between the proton and the neutron in the halo can reveal itself

more strongly in the wave function of the system and give a dominant contribution to the form factor asymptotics (recall that other potentials have substantially larger radii in our three-particle model of ^{6}Li nucleus; consequently, it is natural to assume that they have less influence upon the asymptotics of form factor $F_p(q)$). This assumption allows the form factor $F_p(q)$ to be approximately presented as a product of the form factor $F_{p(d)}(q)$ of the proton in a deuteron and the form factor $F_d(q)$ of the center of masses of the deuteron cluster in ^{6}Li nucleus. Since the motion of the center of masses of the deuteron cluster and the motion of the α-cluster in ^{6}Li nucleus are directly bound with each other (by means of the immovable center of masses of the whole nucleus), we obtain $F_p(q) \approx F_{p(d)}(q)F_d(q) \equiv F_{p(d)}(q)F_\alpha(\frac{m_\alpha}{m_n+m_p}q)$.

Hence, accurate to a rather slowly diminishing multiplier $F_\alpha(\frac{m_\alpha}{m_n+m_p}q)$, the features of the asymptotic behavior of the form factors $F_p(q)$ (in a three-particle system) can resemble the behavior of $F_{p(d)}(q)$ (in a two-particle system). Moreover, the change of a slope of the form factor $F_p(q)$ at $q \approx 5$ Fm^{-1}, which was mentioned above, is associated with the similar behavior of the form factor $F_\alpha(q)$ at $q \approx 10$ Fm^{-1}, and the presence of dips in the form factor $F_p(q)$ can be connected with an infinite number of dips in the form factor $F_{p(d)}(q)$ (shown in Fig. 10 by the dashed curve). Therefore, let us briefly discuss (in more details, it will considered elsewhere) the problem of the asymptotics of a deuteron form factor $F_d(q)$ (in the framework of a potential model and leaving aside the issue of the own form factor of a proton):

$$F_{p(d)}(q) \equiv \int e^{-i(\mathbf{qr})} n_{p(d)}(r) d\mathbf{r} =$$

$$= \int e^{-i\frac{m_n}{m_p+m_n}(\mathbf{qr})} |\varphi_d(r)|^2 d\mathbf{r} =$$

$$= \int \psi_d^*(p)\, \psi_d\left(\left|\mathbf{p} + \frac{m_n}{m_n+m_p}\,\mathbf{q}\right|\right) \frac{d\mathbf{p}}{(2\pi)^3}. \qquad (33)$$

In formula (33), $\varphi_d(r)$ and $\psi_d(q)$ stand for the wave function of the two-particle system (deuteron) in the coordinate and momentum representations, respectively. If the interaction potential in the momentum representation diminishes following the power law $v(p) \underset{p\to\infty}{\longrightarrow} p^{-S}$ (in particular, it is valid for Yukawa potentials), the asymptotics of the wave function at large momenta, as follows directly from the Schrödinger equation, would be $\psi_d(p) \underset{p\to\infty}{\longrightarrow} v(p)/p^2 \sim p^{-(S+2)}$. Then, from expression (33), it would be clear that

$$F_{p(d)}(q) \underset{q\to\infty}{\longrightarrow} \sim \psi_d\left(\frac{m_n}{m_n+m_p}\,q + p_0\right) \sim$$

$$\sim \frac{v\left(\frac{m_n}{m_n+m_p}\,q + p_0\right)}{q^2} \qquad (34)$$

at large transferred momenta as well, which coincides with $v(p)/p^2 \sim p^{-(S+2)}$, in accordance with the results of works [14–18], only in the case of power-law potentials.

However, the estimation $F(q) \sim v(q)/q^2$ does not remain valid for any shape of the potential $v(q)$ (contrary to what was supposed in work [18]). In particular, for potentials with the exponential dependence on the momentum, $v(q) \sim \exp(-\beta q^{1-\varepsilon})$, correct is estimation (34) with the important coefficient $m_n/(m_n+m_p)$ at the transferred momentum which substantially affects the law of form factor decrease. For a potential $v(q)$ that diminishes quicker than the solution $\psi_d(q)$, the asymptotics of $F(q)$ differs considerably from dependence (34), in particular, for Gaussian potentials $v(q) = -g\exp(-aq^2)$. In this case, it can be shown that, in the asymptotic range of large momenta, the form factor of two-particle systems has an asymptotics of type (32) which cannot be reduced to dependence (34). Hence, the form factor asymptotics $F(q) \sim v(q)/q^2$ for power-law (in the momentum representation) potentials does not extend upon all possible potential shapes. Moreover, for potentials with attractive and repulsive gaussoids – in particular, for the triplet potential $V_{np}(r) = 840.545\, e^{-(r/0.44)^2} - 146,046\, e^{-(r/1,271)^2}$, which we use in our model of ^{6}Li nucleus for the description of the interaction between the proton and the neutron – the wave function in the momentum representation is characterized, besides a general decrease, by oscillations as well, which immediately reveals itself in the form factor (the dashed curve in Fig. 10).

Hence, even in the case of two nucleons with Gaussian potentials, the asymptotics of form factors turns out to be nontrivial. For the nuclei examined in this work, we also managed to understand, at a qualitative level, the character of form factor behavior in three-particle systems (in particular, for $F_\alpha(q)$ and $F_p(q)$ discussed above). But the general problem dealing with the asymptotics of form factors in systems more complicated than a two-nucleon one and in the case of Gaussian potentials of interaction between particles remains unresolved.

6. Conclusions

To summarize, we note that variational calculations with Gaussian basis allow the density distribution asymptotics to be analyzed at large (on the nuclear scale) distances. For ^{6}Li and ^{6}He nuclei, the wave functions of which do not differ strongly in the interaction region, we have shown that the asymptotic dependences of density distribution are substantially different (with respect to both halo particles and an α-particle), because these nuclei are characterized by basically different of breakup thresholds (two-particle threshold for ^{6}Li nucleus and three-particle one for ^{6}He one). It was found that at least two competing terms with close exponents in the exponential function are important for the asymptotics of halo nucleon density distribution in ^{6}Li nucleus at large distances. When studying the density distribution of halo neutrons in ^{6}He nucleus, which is characterized by the three-particle breakup threshold, at distances up to several tens of Fm, it is necessary that the second expansion term should be taken into account in addition to the first one, in the expansion of the asymptotics into a $(1/r)$-series, because this term has a considerably larger coefficient.

The analysis of the behavior of charge form factors of ^{6}Li and ^{6}He nuclei at low transferred momenta allowed us to reliably calculate the average quartic radius $\langle r^4 \rangle^{1/4}$. A procedure has been proposed to single out the multipliers $1 - q^2/q^2_{\min}$ from the oscillating form factors and to change over to the expansion of the reciprocal form factor in a q^2-series, which allowed the applicability range of expansions in q^2 to be extended and the quantities $\langle r^2 \rangle^{1/2}$ and $\langle r^4 \rangle^{1/4}$ to be determined from the form factor curves more reliably.

For the form factors $F_\alpha(q)$ and $F_p(q)$, it has been demonstrated that, in the case of Gaussian interaction potentials, the asymptotics of the form factors at large transferred momenta are not of the form $F(q) \sim \left[v(q)/q^2\right]^{A-1}$, as it is stated in the literature (see work [18]).

From the general viewpoint concerning a wide range of interaction potentials and complicated quantum-mechanical systems, a number of problems dealing with form factor asymptotics remains open and requires the additional consideration.

1. B.E. Grinyuk and I.V. Simenog, Yad. Fiz. **72**, 10 (2009).
2. B.E. Grinyuk and I.V. Simenog, Yad. Fiz. Energ. **10**, 9 (2009).
3. Y. Suzuki and K. Varga, *Stochastic Variational Approach to Quantum-Mechanical Few-Body Problems* (Springer, Berlin, 1998).
4. M.V. Kuzmenko and I.V. Simenog, Zh. Fiz. Dosl. (in press).
5. P. Mueller, I.A. Sulai, A.C.C. Villari *et al.*, Phys. Rev. Lett. **99**, 252501 (2007).
6. G. Audi and A.H. Wapstra, Nucl. Phys. A **595**, 409 (1995).
7. B.V. Danilin, S.N. Ershov, and J.S. Vaagen, Phys. Rev. C **71**, 057301 (2005).
8. H. De Vries, C.W. De Jager, and C. De Vries, At. Data Nucl. Data Tables **36**, 495 (1987).
9. P. Egelhof, G.D. Alkhazov, M.N. Andronenko *et al.*, Eur. Phys. J. A **15**, 27 (2002).
10. S.P. Merkuriev, Yad. Fiz. **19**, 447 (1974).
11. L.D. Faddeev and S.P. Merkuriev, *Quantum Scattering Theory for Several Particle Systems* (Kluwer, Dordrecht, 1993).
12. V. Efimov, Yad. Fiz. **12**, 1080 (1970).
13. D.V. Pyatnytskyi and I.V. Simenog, Yad. Fiz. Energ. **10**, 36 (2009).
14. S.D. Drell, A.C. Finn, and M.H. Goldhaber, Phys. Rev. **157**, 1402 (1967).
15. B.M. Karnakov, Yad. Fiz. **19**, 1122 (1974).
16. C. Alabizo and G. Schierholz, Phys. Rev. D **10**, 960 (1974).
17. I.M. Narodetsky, Yu.A. Simonov, and F. Palumbo, Phys. Lett. B **58**, 125 (1975).
18. R.D. Amado and R.M. Woloshyn, Phys. Lett. B **62**, 253 (1976).

Received 26.11.09.
Translated from Ukrainian by O.I. Voitenko

ОСОБЛИВОСТІ АСИМПТОТИК РОЗПОДІЛІВ ГУСТИНИ І ФОРМФАКТОРІВ ЯДЕР ^{6}Li ТА ^{6}He У ТРИЧАСТИНКОВІЙ МОДЕЛІ

Б.Є. Гринюк, І.В. Сименог

Р е з ю м е

Досліджено асимптотики структурних функцій ядер ^{6}Li та ^{6}He у моделі α-частинка плюс два нуклони. Вивчено розподіли густини нуклонів гало та α-частинки на великих відстанях у цих ядрах та проведено порівняння з аналітичними асимптотиками. Запропоновано нове зручне представлення формфактора для малих переданих імпульсів. Проаналізовано проблему асимптотичної поведінки формфакторів. Отримані результати показують, що розвинуті числові схеми варіаційного методу з використанням гаусоїдного базису дозволяють вивчати асимптотичну область структурних функцій як в координатному, так і в імпульсному просторах.